Journal of Ceramic Processing Research. Vol. 10, No. 6, pp. 774~779 (2009)

J O U R N A L O F
Ceramic Processing Research

Simultaneous synthesis and consolidation of a nanostructured 4Fe-Al_2O_3 composite from mechanically activated powders by high frequency induction heated sintering

Na-Ra Park[a], Seong-Hyeon Jeon[a], Je-Shin Park[b], Wonbaek Kim[b] and In-Jin Shon [a,c]*

[a]*Division of Advanced Materials Engineering and the Research Center of Advanced Materials Development, Engineering College, Chonbuk National University,Chonbuk, 561-756, Republic of Korea*

[b]*Minerals and Materials Processing Division, Korea Institute of Geoscience and Mineral Resources, Daejeon, Republic of Korea*

[c]*Department of Hydrogen and Fuel Cells Engineering, Specialized Graduate School, Chonbuk National University,Chonbuk, 561-756, Republic of Korea*

A nanocrystalline 4Fe-Al_2O_3 composite was simultaneously synthesized and consolidated by a high frequency induction heated sintering method within 2 minutes from mechanically activated powders of Fe_2O_3 and 2FeAl. The average grain sizes of Fe and Al_2O_3 were 72 and 43 nm, respectively. The mechanical properties of the composite were investigated.

Key words: Rapid Synthesis, Composite, Nanostructured composite, Mechanical properties, Fe-Al_2O_3.

Introduction

The continuous increase in the performance requirement of materials for aerospace and automotive applications has lead to the development of several structural composite materials. Among these, metal matrix composites refer to a type of material in which rigid ceramic reinforcements are embedded in a ductile metal or alloy matrix. Metal matrix composites combine metallic properties (ductility and toughness) with ceramic characteristics (high strength and modulus), leading to greater strength in shear and compression and to higher service temperature capabilities. The attractive physical and mechanical properties that can be obtained with metal matrix composites, such as high specific modulus, strength-to weigh ratio, fatigue strengh, and temperature stability and wear resistance, have been documented extensively [1-6]

Traditionally, discontinuously reinforced metal matrix composites have been produced by several processing routes such as powder metallurgy, spray deposition mechanical alloying, various casting techniques and SHS (self-propagating high temperature synthesis). All these techniques are based on the addition of ceramic reinforcements to the matrix materials which may be in molten or powder form. One of these techniques, SHS developed by Merzhanov and coworkers [7, 8] in the late 1960s, refers to a process in which materials with sufficiently high heat of formation are synthesized in a combustion wave, which after ignition, spontaneously propagates throughout the reactants and converts them into the products. SHS is extremely attractive, givings a highpurity product due to the volatilization of low boiling point impurities at elevated temperature, and high productivity due to very high reaction rates.

Nanocrystalline materials have received much attention as advanced engineering materials with improved physical and mechanical properties [9, 10]. As nanomaterials possess high strength, high hardness, excellent ductility and toughness, much attention has been paid to the application of nanomaterials [11, 12]. In recent days, nanocrystalline powders have been developed by the thermochemical and thermomechanical process termed as the spray conversion process (SCP), co-precipitation and high energy ball milling [13-15]. However, the grain size in sintered materials becomes much larger than that in the pre-sintered powders due to the rapid grain growth during the conventional sintering process. Therefore, even though the initial particle size is less than 100 nm, the grain size increases rapidly up to 500 nm or larger during the conventional sintering [16]. So, controlling grain growth during sintering is one of the keys to the commercial success of nanostructured materials. In this regard, the high frequency induction heated sintering method which can make dense materials within 2 minutes, has been shown to be effective in achieving this goal [17, 18].

The purpose of this study is to produce a dense nanocrystalline 4Fe-Al_2O_3 composite within 2 minutes from mechanically activated powders using this high frequency induction heated combustion method and to evaluate its mechanical properties (hardness and fracture toughness).

Experimental procedure

Powders of 99% Fe_2O_3 (< 5 μm, Aldrich) and 99%

*Corresponding author:
Tel : +82 63 270 2381
Fax: +82 63 270 2386
E-mail: ijshon@chonbuk.ac.kr

pure FeAl (< 300 μm, Sinagigong, Inc) were used as starting materials. Fe_2O_3 and 2 FeAl powder mixtures were first milled in a high-energy ball mill, Pulverisette-5 planetary mill with 250 rpm and for 10 h. Tungsten carbide balls (8 mm in diameter) were used in a sealed cylindrical stainless steel vial under an argon atmosphere. The weight ratio of ball-to-powder was 30 : 1. Milling resulted in a significant reduction of grain size. The grain sizes of Fe and Al_2O_3 were calculated by Suryanarayana and Grant Norton's formula [19] :

$$B_r\,(B_{crystalline} + B_{strain})\cos\theta = k\lambda/L + \eta\sin\theta \quad (1)$$

where B_r is the full width at half-maximum (FWHM) of the diffraction peak after instrumental correction; $B_{crystalline}$ and B_{strain} are the FWHM caused by the small grain size and internal stress, respectively; k is constant (with a value of 0.9); λ is the wavelength of the X-ray radiation; L and η are the grain size and internal strain, respectively; and θ is the Bragg angle. The parameters B and B_r follow Cauchy's form with the relationship: $B = B_r + B_s$, where B and B_s are the FWHM of the broadened Bragg peaks and the standard sample's Bragg peaks, respectively.

After milling, the mixed powders were placed in a graphite die (outside diameter, 45 mm; inside diameter, 20 mm; height, 40 mm) and then introduced into the induced current activated sintering system made by Eltek in South Korea, shown schematically in Fig. 1. The four major stages in the synthesis are as follows. Stage 1-Evacuation of the system. Stage 2-Application of the uniaxial pressure. Stage 3-Heating of the sample by the induced current. Stage 4-Cooling of sample. The process was carried out under a vacuum of 40 mtorr (5.33 Pa).

The relative densities of the synthesized sample measured by the Archimedes method are over 95% of the theoretical value. Microstructural information was obtained from product samples which were polished at room temperature.

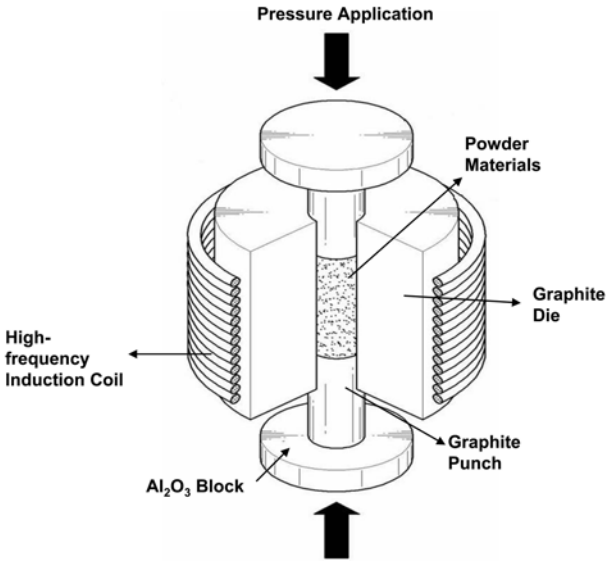

Fig. 1. Schematic diagram of the apparatus for high frequency induction heated sintering.\

Compositional and microstructural analyses of the products were made through X-ray diffraction (XRD) and scanning electron microscopy (SEM) with energy dispersive X-ray analysis (EDAX). Vickers hardness was measured by performing indentations at a load of 30 kg and a dwell time of 15 s on the synthesized samples.

Results and Discussion

X-ray diffraction results from the raw powders and high energy ball milled powders is shown in Fig. 2. The reactant powders of Fe_2O_3 and FeAl were detected but products, Fe and Al_2O_3, were not detected in Fig. 2(c). From the above result the mechanical alloying did not occur during the milling. The full width at half-maximum

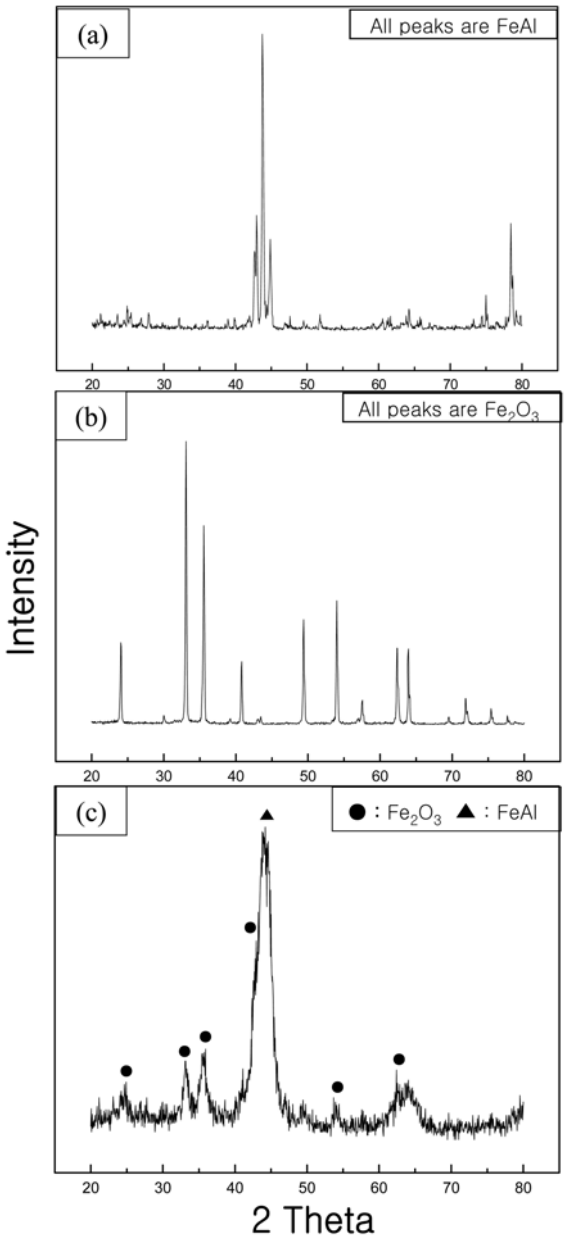

Fig. 2. XRD patterns of raw materials and mechanically activated powder : (a) Al, (b) Fe_2O_3 and (c) mechanically activated powder.

(FWHM) of the diffraction peak of milled powders is wider than that of the raw powders due to the strain and refinement of the powder. The average grain sizes of Fe_2O_3 measured by Suryanarayana and Grant Norton's formula are about 34 nm. A SEM image and X-ray mapping of milled powders are shown in Fig. 3. The powders (FeAl, Fe_2O_3) are uniformly distributed from the X-ray mapping results [Fig. 3 (b), (c) and (d)]. The variations in shrinkage displacement and temperature of the surface of the graphite die with heating time during the processing of the 2FeAl and Fe_2O_3 system are shown Fig. 4. As the induced current was applied, shrinkage displacement gradually increased and then remarkably increased at the lower temperature of 550 °C. X-ray diffraction patterns of sample of (a) after milling, (b) just before abrupt increase of shrinkage and (c) heated to 900 °C are shown in Fig. 5. The product

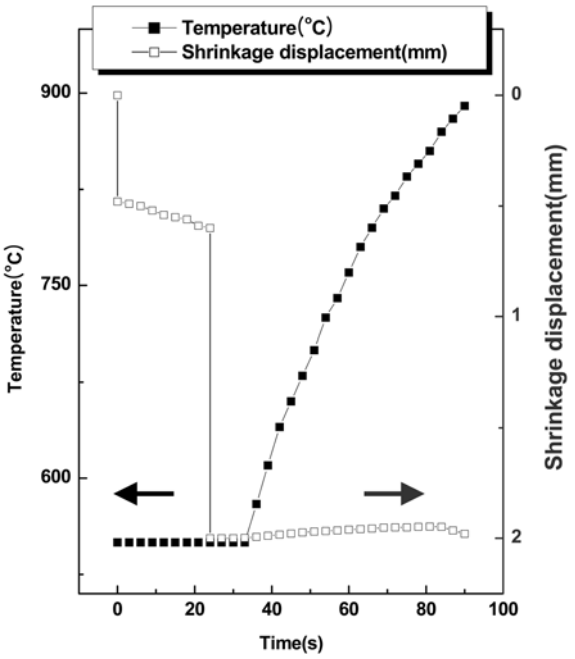

Fig. 4. Variation of temperature and shrinkage displacement with heating time during high frequency induction heated sintering of 2FeAl + Fe_2O_3.

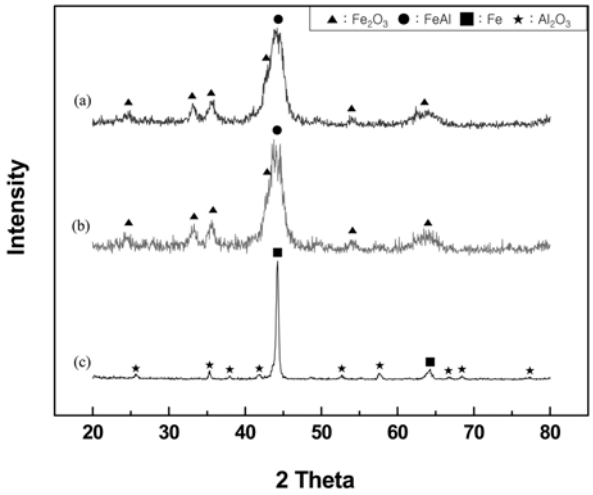

Fig. 5. XRD patterns of the 2FeAl + Fe_2O_3 system : (a) after milling, (b) before combustion synthesis, (c) after combustion synthesis.

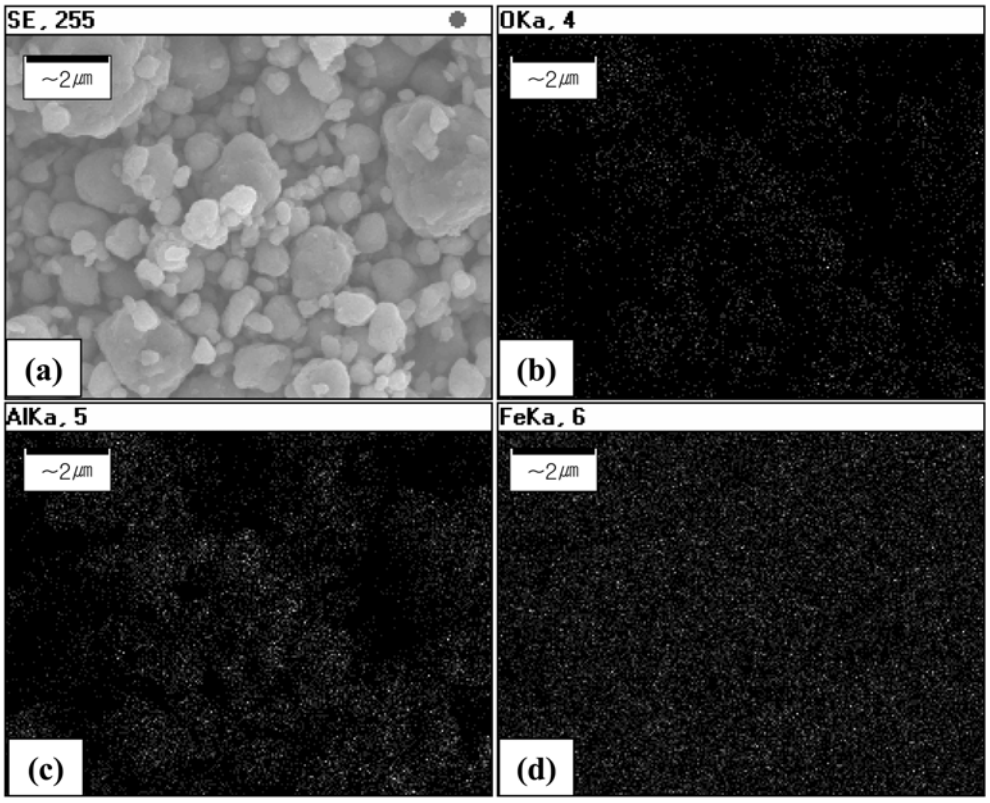

Fig. 3. SEM image and X-ray mapping of FeAl and Fe_2O_3 powders : (a) SEM image, (b) oxygen mapping, (c) aluminum mapping, (d) iron mapping.

(Fe, Al_2O_3) was not detected in Fig. 5(a) and (b) but detected in Fig. 5(c). Fig. 6 shows the plot of the B_r ($B_{crystalline} + B_{strain}$) cosθ versus sinθ of Fe and Al_2O_3 in the sintered composite. The structural parameters, i.e. the average grain sizes of Fe and Al_2O_3 obtained from the X-ray data by Suryanarayana and Grant Norton's formula [19], were 72 nm and 43 nm, respectively. A SEM image of the sample heated to 900 °C and X-ray mappings are shown in Fig. 7. The Al_2O_3 particles(dark phase) were well distributed in the matrix, as seen from the SEM image and X-ray mapping shown in Fig. 7. The abrupt increase in the shrinkage displacement at the ignition temperature in Fig. 4 is due to the increase in density resulting from the change in the molar volume associated with the formation of 4 Fe-Al_2O_3 from the reactants (2FeAl and Fe_2O_3) and the consolidation of the product. It is considered that the composite is synthesized at a lower temperature because the raw powders are activated during the high energy ball milling which makes powder

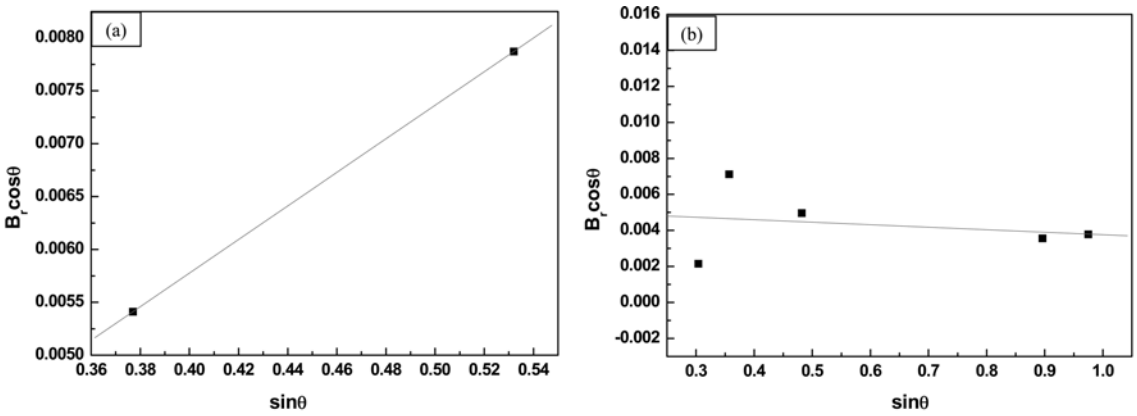

Fig. 6. Plot of the B_r ($B_{crystalline} + B_{strain}$) cosθ versus sinθ of Fe (a) and Al_2O_3 (b) in the sintered composite.

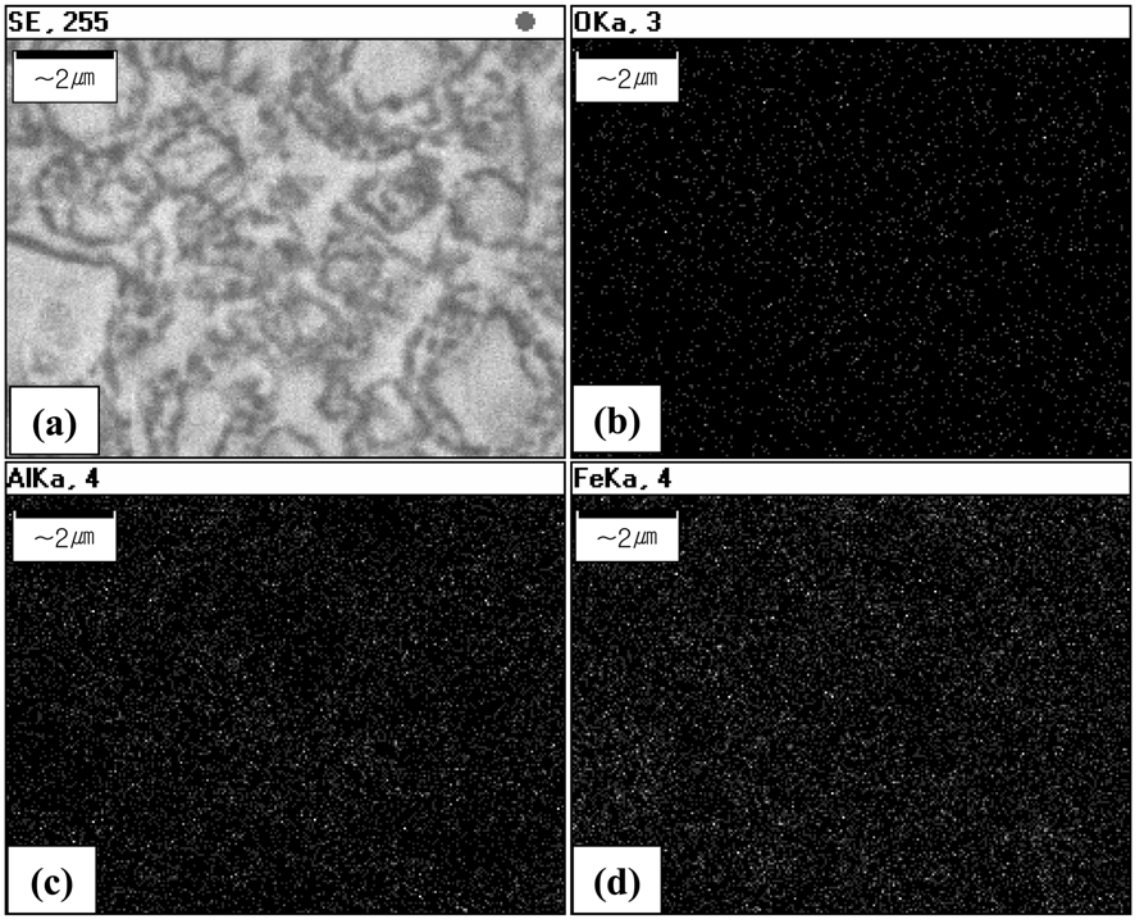

Fig. 7. Scanning electron microscope image and X-ray mapping of 4Fe-Al_2O_3 composite : (a) SEM image, (b) oxygen mapping, (c) aluminum mapping, (d) iron mapping.

with strain and defects.

Vickers hardness measurements were made on polished sections of the 4 Fe-Al_2O_3 composite using a 30 kgf load and 15 s dwell time. The calculated hardness value of 4 Fe-Al_2O_3 composite was 730 kg/mm^2 (7,158 MPa). This value represents an average of five measurements. Indentations with large enough loads produced median cracks around the indent. From the length of these cracks, fracture toughness values can be determined using two expressions. The first expression, proposed by Anstis *et al*. [20] is :

$$K_{IC} = 0.016(E/H)^{1/2} \cdot P/C^{3/2} \quad (2)$$

where E is Young's modulus, H the indentation hardness, P the indentation load, and C the trace length of the crack measured from the center of the indentation. The modulus was estimated by the rule mixtures for the 0.48 volume fraction of Al_2O_3 and the 0.52 volume fraction of Fe using E(Al_2O_3) = 380 GPa [21] and E(Fe) = 211 Gpa [22]. The second expression, proposed by Niihara *et al*. [23, 24], is

$$K_{IC} = 0.023(c/a)^{-3/2} \cdot H_v \cdot a^{1/2} \quad (3)$$

where c is the trace length of the crack measured from the center of the indentation, a the half of average length of two indent diagonals, and H_v the hardness.

As in the case of hardness values, the toughness values were derived from the average of five measurements. The toughness values obtained by the two methods of calculation are 9.7 and 9 MPa·m$^{1/2}$, respectively. The hardness and fracture toughness of Al_2O_3 with grain size of 4.5 μm are reported as 1800 kg/mm^2 (17,651 MPa) and 4 MPa·m$^{1/2}$, respectively [21]. The hardness of 4Fe-Al_2O_3 composite is lower than that of monolithic Al_2O_3 but the fracture toughness is higher than the value of Al_2O_3 due to the addition of ductile Fe.

A typical indentation pattern for 4Fe-Al_2O_3 composite is shown in Fig. 8. Typically, one to three additional cracks were observed to propagate from the indentation corner. A higher magnification view of the indentation median crack in the composite is shown in Fig. 8(b). This shows the crack was deflected and Fe was plastically deformed at arrows.

Conclusions

Using the high frequency induction heated sintering method, the densification of a nanostructured 4Fe-Al_2O_3 composite was accomplished from mechanically activated powders (Fe_2O_3 and 2FeAl). Complete densification can be achieved within 2 minutes. The relative density of the composite was 95% for an applied pressure of 80 MPa and the induced current. The composite was synthesized at temperature lower than 550 °C because raw powders are activated during the high energy ball milling. The average grain sizes of Fe and Al_2O_3 prepared by HFIHS were about 72 nm and 43 nm, respectively.

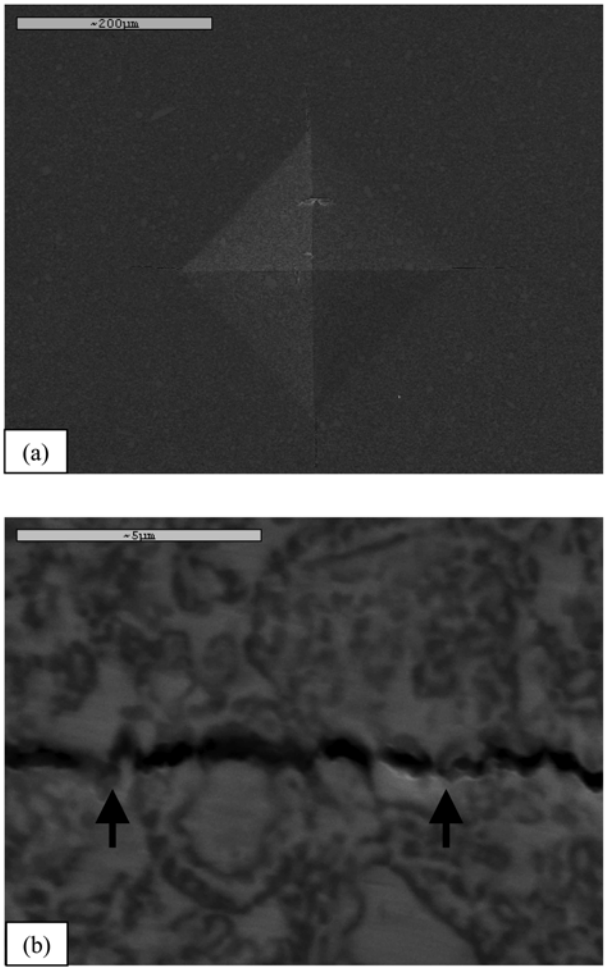

Fig. 8. Vickers hardness indentation (a) and median crack propagating (b) of 4Fe-Al_2O_3 composite.

The average hardness and fracture toughness values obtained were 730 kg/mm^2 (7,158 MPa) and 9.7 MPa·m$^{1/2}$, respectively.

Acknowledgment

This study was supported by a grant from basic research project of Korea Institute of Geoscience and Mineral Resources.

References

1. L. Ceschini, G. Minak and A. Morri, Composites Science and Technology , 66 (2006) 333-339.
2. S.C. Tjong and Z.Y. Ma, Materials science and Engineering, 29 (2000) 49-55.
3. D.J. Lloyd, Particle reinforced aluminum and magnesium metal matrix composites, Int Mater Rev 39[1] (1994)1-29.
4. J.M. Torralba and F. Velasco, P/M aluminum matrix composites : an overview, J Mater Process Technol 133[1-2] (2003) 3-206.
5. R. Fan, B. Liu, J. Zhang, J. Bi and Y. Yin, Mater. Chem. Phys. 91 (2005) 40-46.
6. Jose S. Moya, Sonia Lopez-Esteban, Carlos Pecharroman,

The challenge of ceramic/metal microcomposites and nanocomposites Progress in Materials Science 52 (2007) 1017-1027.
7. I.P. Borovinskaya, A.G. Merzhanov, N.P. Novikov and A.K. Filonenko, Combust. Explos. Shock Waves 10 (1974) 2-10.
8. A.G. Merzhanov, G.G. Karyuk, I.P. Borovinskaya, V.A. Prokudina and E.G. Dyad, Sov. Powder Metall. Met Ceram. 20 (1981) 709-715.
9. M.S. El-Eskandarany. J. Alloys & Compounds 305 (2000) 225-230.
10. L. Fu, LH. Cao and YS. Fan, Scripta Materialia, 44 ,1061 (2001)
11. K. Niihara, Nikahira, Elsevier Scientific Publishing Co., Trieste, Italy (1990)
12. S. Berger, R. Porat and R. Rosen. Progress in Materials 42 (1997) 311-330.
13. I.J. Shon, D.K. Kim, I.Y. Ko, J.K. Yoon and K.T. Hong, Materials Science Forum 534-536 (2007) 525-530.
14. Z. Fang and J.W. Eason. Int. J. of Refractory Met. & Hard Mater. 13 (1995) 297-303.
15. A.I.Y. Tok, l.H. Luo and F.Y.C. Boey, Matrials Science and Engineering A 383 (2004) 229-235.
16. M. Sommer, W.D. Schubert, E. Zobetz and P. Warbichler, Int. J. of Refractory Met. & Hard Mater. 20 (2002) 41-46.
17. H.C. kim, I.J. Shon, I.J. Jeong, I.Y. Ko, J.K. Yoon and J. M. Doh, Metals and Materials International 13 (2007) 39-45.
18. H.C. Kim, I.J. Shon, I.K. Jeong and I.Y. Ko, Metals and Materials International, 12 (2006) 393-398.
19. C. Suryanarayana and M. Grant Norton, X-ray Diffraction A Practical Approach, Plenum Press, (1998) p.213
20. G.R. Anstis, P. Chantikul, B.R. Lawn and D.B. Marshall, J. Am. Ceram. Soc. 64 (1981) 533-540.
21. Mohamed N. Rahaman, Aihua Yao, J. Am. Ceram. Soc., 90[7] (2007) 1965-1988.
22. http://en.wikipedia.org/wiki/Elastic properties of the elements (data page)
23. K. Niihara, R. Morena and D.P.H. Hasselman, Evaluation of KIC of Brittle Solids by the Indentation Method with Low Crack-to-Indent Ratios, J. Mater. Sci. Lett. 1, (1982) 12-16.
24. D.Y. Oh, H.C. Kim, J.K. Yoon and I.J. Shon, J. Alloys & Compound 395 (2005) 174-179.